RESEARCH ARTICLE OPEN ACCESS

Compensating Ship Deck Movement under Influence of Wind Waves Using 6 DOF Stewart Platform

Dabbiru Ravi Vikranth [1], Dr. Anurag Sarma [2], Dr. Brijesh Patel [3]

Research Scholar [1], Department of Comp. Science & Engineering, MATS University, Raipur
Professor [2], Department of Comp. Science & Engineering, MATS University, Raipur
Professor [3], Department of Aeronautical Engineering, MATS University, Raipur

ABSTRACT

Several wave motions (sea wind waves, swell waves etc.) have a considerable effect on smaller ships in comparison to their bigger counterparts. Safe Landing on Ship Deck Platform is a herculean task owing to dynamic nature of heave, pitch and roll motions of the ship causing unmanageable deck motion/ state estimation for safe landing, handling of sensitive objects etc. The Project aims at compensating the motion of the ship by using a Stewart platform. It is a parallel platform operated by actuators mimicking the heave, pitch and roll motions of the ship deck. A compensating mechanism is designed by keeping upper plate stable irrespective of the motion of the base plate or ship. This is achieved by applying Sine Summation Fit Algorithm to the incoming wind hitting along the bow, stern, port, starboard or cross sides of the ship. The Corrected Sine Summation Fit Algorithm in all 6DOF is computed and thereby Root Mean Square Error (RMSE) corrected algorithm is obtained. The RMSE algorithm is fed as input to the servo motors of Stewart Platform. The motion thus obtained keeps the Stewart platform or ship deck platform fairly stable with $\pm 5^0$ roll, $\pm 5^0$ pitch and sway restricted/ compensated in experimental setup. Experimentation is performed using Arduino MEGA 2560, MPU6050 and gyroscopic sensors, actuator, and microcontrollers. The scaled model consists of servo motors as rotary actuators and on experimentation, it is found that it can compensate the pitch and roll of base plate by an angle of about ±20˚ satisfactorily. It can be used as stable platform for launching and recovery of Unmanned Aerial Vehicles (UAV) and can be used by creating a stable bridge for transportation of men and machinery aboard/ from autonomous system.

***Keywords* :-** Sine Summation Fit Algorithm, RMSE algorithm, Stewart Platform, 6DOF, Arduino MEGA 2560, Breadboard, MPU6050, Rod end etc.

I. INTRODUCTION

Linear motions like heave, surge & drift and angular motions like pitch, roll & yaw are experienced by floating bodies as shown in Figure 1. Hydrostatic/ Hydrodynamic equations of motion for buoyant bodies can be developed by using Lagrange's equation or Newton's second law. Second method employs the total summative hydro-dynamic pressure acting on the ship's contact surface [i.e. platform and sides] to derive the external forces and moments. Of the six motions of the ship, the roll oscillations dictate the status of ship being capsized or not. At smaller roll angles, the ships response can be given by a linear equation. With increase in oscillating amplitude, non-linear effects are encountered. The non-linearity is due to type of supportive damping and moment. Non-linearity can magnify small deviations, which aid in triggering to the point where the restoring force contribute to capsizing. Since ship capsizing directly proportional to the roll angle, a precise estimation of roll is crucial in order to predict ship motion. The prediction of ship deck motion is of interest to pilots of Remotely Piloted Vehicles (RPV) due to the difficulty of landing aircraft on a moving ship deck. The sudden motion of the ship deck can cause increased wear & tear to landing gear, may require multiple landing attempts, and even may result in the loss of an aircraft. An accurate prediction of the motion of the ship would mitigate some of the risk associated with landing on an aircraft carrier.

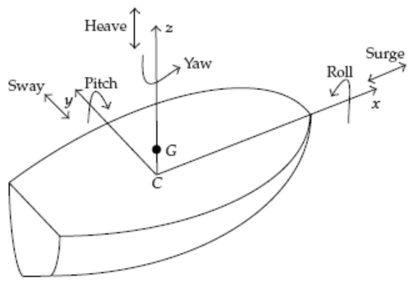

Figure 1: Ship schematic diagram showing the six degrees of freedom.

Understanding the landing conditions requires an accurate prediction of how the aircraft carrier will move in the future. Ship deck motion is a combination of the harmonic forces generated by ocean waves and the dynamic response of the ship [1]. These phenomena combine to produce the final motion of the ship deck. Any movement off the sea can produce pitch, roll, yaw, and/or heave at the ship deck platform. Different sea conditions make ships behave in different manners due to their hull design, size, stabilization systems etc. An RPV operating at such platforms must observe heave, pitch, and roll motion of the landing platform and determine landing contact time based on human timing reaction as well as aircraft performance.

Nature of Sea Waves:
Ocean waves are divided into two main categories: sea and swell [5]. Sea is defined as a train of waves driven mostly by the local wind conditions. Swell refers to the leftovers of a wave that has disseminated from the original generated source area [5] Swell has longer wavelengths and a more predictable height than sea. Surface waves are a combination of both swell and wind waves, both of which are in constant flux, and therefore can potentially consist of an infinite number of harmonic waves.

A ship structure adds its own dynamic straits to the ocean wave, the resultant waves can be measured by onboard ship sensors as shown in Fig. 2. The combination of ship and ocean waves though can be complex, the total response can be expressed as a summation of sine waves with amplitudes, phase angles, coordinate directions, and frequencies [2]

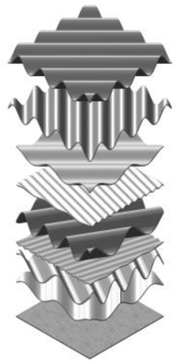

Fig 1:3d representation of ship deck motion

Many approaches are considered and studied to predict ship deck motion. Emphasis is laid on time-series analysis to predict ship motion employing Auto Regressive (AR) and Moving Average Auto Regressive (ARMAX), as well as Kalman filters, Wiener filters, and the Volterra model.Artificial Intelligence based .

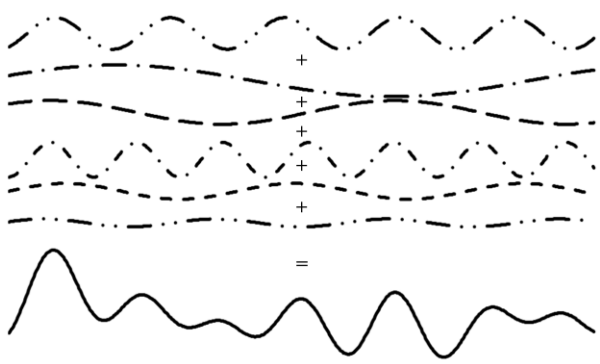

Fig. 2. Two-dimensional representation of ship deck motion.

Propagation methods (Neural Networks) are used viz. Wavelet Neural Network (WNN), Minor Component Analysis (MCA), Extreme Learning Machines (ELM) etc. This paper uses sine-summation method to predict ship motion. The algorithm fits a Sine waves summation to original ship dataset and projects the summation onto prospective time slots (future).

Acceleration data collected aboard ships can be used along with the proposed method to make predictions onboard the vessel. The prediction can then be transmitted to the Unmanned Aerial Vehicle (UAV) in advance of a landing attempt to indicate the suitability of landing within the projected time frame. An RPV could then use the prediction based on original dataset to determine if there exists an ideal landing speed and descent trajectory in the next several seconds, and the decision could be made to touch down immediately or make another attempt later.

II.SHIP MOTION

A ship has 6DOF with translational and rotational components depicted in Fig. 3. The coordinate system is being assumed in the following format;

- X-axis points towards the bow side or front side of the ship,
- Y-axis points towards the port side of the ship,
- Z-axis points towards the observing sky or top side of the ship.

Movement in the translational (x, y, z) directions are defined as surge, drift, and heave respectively. The Rotational motions along (x, y, z) directions are roll, pitch, and yaw respectively. In terms of the body-fixed coordinate system, and the ship motion by rigid body displacement method; thus equations of motion can be expressed using Newton's second law in vector notation as;

$$F_S + W = \frac{d}{dt}(mV) + \omega(mV) \qquad (1)$$

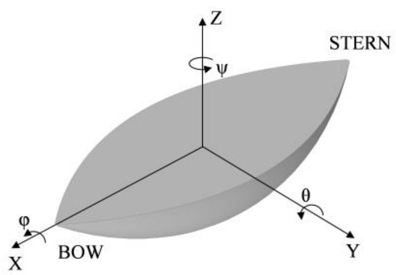

Fig. 3. Accepted ship motion model with six degrees of freedom.

and

$$M_S = \frac{d}{dt}([I]\,\omega + \omega \times ([I]\,\omega)) \quad (2)$$

The translational rigid-body motion is governed by (1) while the rotational motion is governed by (2). These two equations together express the complete rigid-body motion of the ship in all six degrees of freedom. Each degree of freedom in ship motion can be visualized as spring-mass-damper system subject to a harmonic forcing function [3]. For any arbitrary degree of freedom x, the differential equation of motion for a spring mass-damper can be written as;

$$m = \frac{d^2x}{dt^2} + c\frac{dx}{dt} + kx = F\sin(\omega t) \quad (3)$$

the harmonic forcing function is composed of only a single sine wave. Due to the coupling between various degrees of freedom in the system, spring mass damper system does not represent each degree of freedom. The coupling effects between each degree of freedom can be considered part of the forcing function on the right-hand side of (3) or as a disturbance to the system. Solving (3) for the position as a function of time and assuming that the elastic modes of the ship contribute very little to the motion of the ship, the equation yields;

$$x(t) = C_1e^{\lambda}1^t + C_2e^{\lambda}2^t + A_f(F/k)\sin(\omega t - \phi_0) \quad (4)$$

The first two terms on the right-hand side correspond to the motion of the ship governed by its self dynamic response. The last term is the contribution of the ocean waves and coupling effects from other degrees of freedom to the resultant ship deck motion.

The first two terms describe the ship's dynamic contributions to the resultant ship motion, while the last term describes the contribution of the harmonic force of the ocean waves. Assuming that the dynamic motion of the ship is oscillatory or that the forcing function is much greater than the first two terms, the resultant motion can be represented by a combination of the dynamic motion of the ship and the forcing function of the ocean.

III. SINE-SUMMATION PREDICTION METHOD

Ship motion can be approximated by a summation of harmonic waves. A simple harmonic wave can be represented as an array of [amplitude, frequency, phase shift, damping coefficient, and constant offset], which is given by formula;

$$Ae^{-\lambda t}\sin(\omega t + \phi_0) + z \quad (5)$$

Due to the relatively small effect that damping has over a short period of time on a large, and especially on slow-moving ship - the damping factor can be ignored [3] [5] and (5) can be rewritten as

$$A\sin(\omega t + \phi_0) + z \quad (6)$$

When large no. of sine waves are used, the past ship motion data could be described exactly; however, at some point the number of sine waves must be truncated. The proposed method constructs a sine wave summation iteratively by adding a single sine wave per iteration and minimizing the root mean square error (RMSE) between the past ship motion data and the sine summation approximation. There are two distinct components present in the method: a start-up procedure and a real-time algorithm. The proposed method requires a dataset having holding time and motion data for a single degree of freedom and the data range over which the fit is scheduled to be made.

Step I. Determining Harmonic Components

There are four datasets viz. the original dataset (or simply the dataset), the actual ship motion data, the prediction, and the sine-summation fit. The original dataset and the actual ship motion data are both found using the ship's sensors. The original data is data that the ship has gathered in the past, and the actual motion is that which is obtained after the algorithm starts. The sine-summation fit is a fit of the original dataset made by the algorithm, while the prediction represents the prediction of the actual ship motion generated by the algorithm.

The first iteration attempts to fit the original dataset using a single sine wave. The input to the dataset is [amplitude, frequency, phase angle, and constant offset]. A fast Fourier transform (FFT) is performed on the dataset, which divides the acceleration into its frequency components according to their effect. The power spectrum is then calculated;

$$Pxx = |FFT^2|\,\delta t^2 \quad (7)$$

where δt is the time interval in the dataset [2]. In addition to frequency information, the output of the FFT is used to find relative amplitude and phase shift associated with each frequency component, which can be accomplished using;

$$SA = (\sqrt{2})(\sqrt{[real[FFT]^2 + imag\,[FFT]^2]}/N \quad (8)$$

for the amplitude spectrum, and

$$SP = \arctan\left(\frac{imag\,[FFT]}{real\,[FFT]}\right) \quad (9)$$

for the phase spectrum [2].

Each spectrum is found within the same frequency domain, and can therefore link the most influential frequency with a corresponding amplitude and phase angle. The phase angles given by the phase spectrum represent the phase shift relative to the starting of the time domain, in the range from $-\Pi$ to $+\Pi$. The most influential frequency is chosen along with the corresponding amplitude and phase shift to be used as initial guesses for the harmonic parameters of the first sine wave. The amplitude spectrum for the original dataset, found using the FFT, contains only positive values. Due to the inclusion of a phase shift, ϕ_0, there is no need to use a negative amplitude. An estimate for the constant offset is determined by taking the average value of the dataset being analyzed.

Step II. Down-sample the Dataset

To reduce the computational complexity of the optimization is used as shown in Step III, the original dataset is down-sampled using the shortest wave

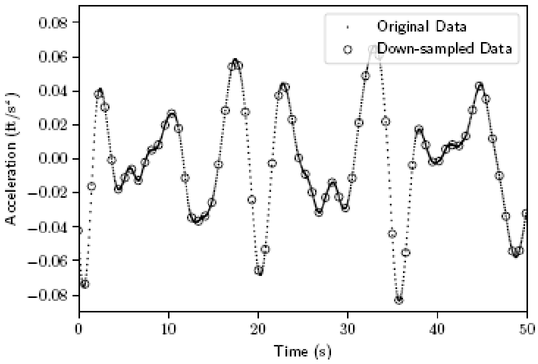

Fig. 4. Effect of down-sampling with four data points per minimum period on a dataset.

period as a benchmark. The shortest wave period is found by extracting from the power spectrum the highest frequency component that will be used in the sine-summation fit and calculating the period using

$$T_{min} = \frac{2\Pi}{\omega_{max}} \qquad (10)$$

If the number of sine waves that will be used to create the sine-summation fit is 'n', then the set of highest 'n' frequencies will be found according to their influence, and the highest frequency (i.e. that with the lowest influence) from that set will be taken as ω_{max}. The algorithm may also be run until adding another sine wave to the sine summation fit doesn't appreciably change the RMSE. The Nyquist frequency can be calculated using the sampling frequency, fs,

$$f_{Nyquist} = fs/\, 2 \qquad (11)$$

The Nyquist frequency can then be taken as ω_{max} after being converted to units of rad/ s. The dataset is down-sampled by taking four data points for every minimum period as shown in Fig. 4. This allows the frequency components present in the dataset to be preserved while increasing the algorithm speed and reducing the space complexity. Taking four data points provides a conservative approach to down-sampling; as only two data points are sufficient for every minimum period. Four data points are kept to ensure that even high frequency datasets are accurately characterized after down-sampling.

Step III. RMSE Optimization of the Sine Summation

The optimization of the sine wave is accomplished by adjusting the harmonic parameters in (6) to minimize the RMSE. The RMSE is calculated as

$$RMSE = \sqrt{(\sum_{1}^{N} ([(\acute{c} - c)^{2]}/ N))} \qquad (12)$$

where ć represents the value of the sine-summation fit and c represents the value of the dataset. The Broyden-Fletcher-Goldfarb-Shanno (BFGS) gradient descent method is used to minimize the RMSE.

Step IV. Sum the Sine Waves and Calculate the Fit Error

The optimized harmonic parameters found in Step III were stored and they are used as the initial guesses for the next iteration of the start-up procedure. As additional sine waves are added to the sine-summation fit, they are summed together to form the fit of the original dataset.

The optimized sine wave from the first iteration is subtracted from the original dataset to find the error of thefit, which is used by the FFT in the next iteration. The fit error retains all the frequency information of the original dataset, excluding the frequencies that are extracted.

While the initial guesses for the harmonic parameters are obtained using an FFT on the fit error of the previous iteration, the optimization minimizes the RMSE between the fit and the original dataset, not the fit error. Each iteration adds three additional harmonic parameters (composing a full sine wave without a constant offset) to be optimized. The harmonic parameters from previous iterations were already optimized, so they change very little in future iterations.

Steps I through IV can be repeated until the RMSE between the sine-summation fit and the original dataset change by less than a threshold value or until a predetermined number of sine waves had been generated. The final form of the sine-summation approximation is

$$f(t) = \sum_{n=1}^{N} A_n \sin(\omega n + \phi_{0n}) + z \qquad (13)$$

Figure 5 shows an example of Steps I - IV of the start-up procedure progressing through three iterations. As more sine waves are added, a better approximation of the original dataset is achieved. This can be seen in Fig. 6, where 14 sine waves were used in the fit.

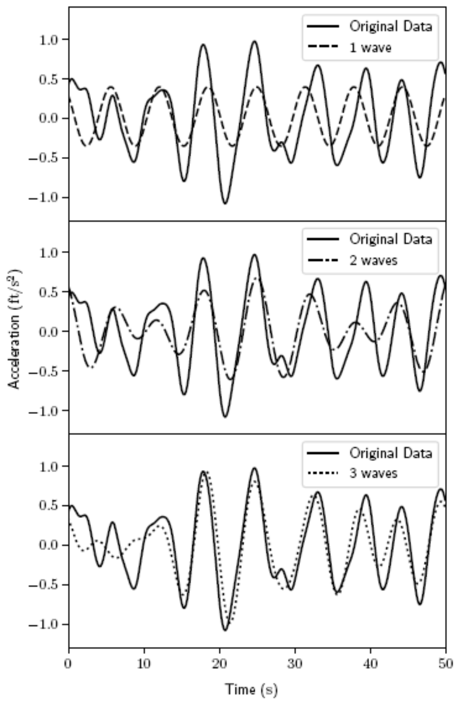

Fig. 5. The sine-summation process using three sine waves to fit a dataset.

Step V. Project the Sine Summation

Once the given number of sine waves has been generated using Steps I through IV, the sine-summation fit is projected into the future by some time interval. This prediction is then compared to the actual ship motion to compute the RMSE. The RMSE of the prediction is reported in both dimensional and non dimensional forms. The dimensional form of the RMSE is used to more easily make comparisons between different prediction methods, which often express results in terms of a dimensional RMSE value. The non dimensional RMSE normalizes the RMSE values for more accurate comparisons when dealing with high-amplitude datasets. The proposed algorithm normalizes the prediction RMSE by the maximum value in the original dataset to non dimensionalize the RMSE.

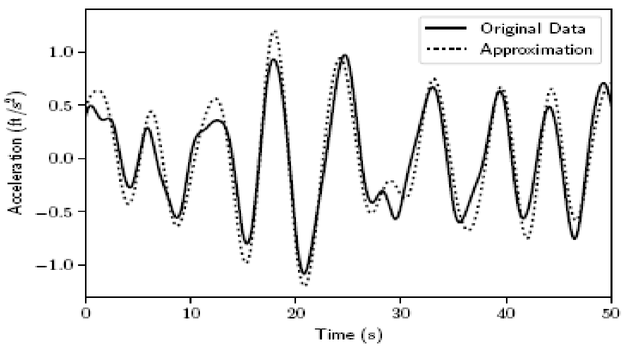

Fig. 6. The final sine-summation fit of the original data using 14 sine waves.

Real-Time Implementation

As mentioned previously, real-time capabilities have been developed for the proposed algorithm. After running the start-up procedure with a given number of sine waves over a specific dataset, the final amplitudes, frequencies, phase shifts and offset are stored along with the amount of time taken to perform the analysis. This computational time is then used to shift the original dataset, which allows the algorithm to stay updated with the data collected in real-time by the sensors on the ship.

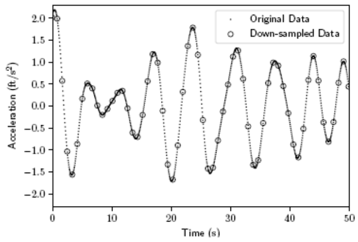

Fig. 7. Heave data down-sampled at four points per minimum period.

After shifting the data, Step III is performed again with all the harmonic parameters from the first analysis used as initial guesses. The maximum number of iterations performed by the optimization routine is drastically reduced during the analysis over the shifted dataset, since relatively few data points are added to the dataset. In a practical case, the startup procedure could be initiated several minutes before the aircraft attempts to land and transition into the real-time updates to provide more timely predictions for the pilot.

Inverse Kinematics of Stewart Platform

The Stewart Platform consists of 2 rigid frames connected by 6 variable length legs. The Platform is considered as the reference frame work, with orthogonal axes x', y', z'. The Base has its own orthogonal coordinates x, y, z. The Base has 6 DOF with respect to the Platform. The origin of the Base coordinates can be defined by 3 translational displacements with respect to the Platform, along each one for each axis. Three angular displacements then define the orientation of the Base with respect to the Platform. A set of Euler angles are used in the following sequence:

a) Rotate an angle ψ (yaw) around the z-axis
b) Rotate an angle θ (pitch) around the y-axis
c) Rotate an angle Φ (roll) around the x-axis

A) First Rotation ψ (yaw) around the z-axis

There is a particular point P on the base plate and getting yaw angle Ψ with respect to z- axis.

$$x' = OA - BC$$
$$= x\cos\Psi - y\sin\Psi$$
$$y' = AB + CP$$
$$= x\sin\Psi + y\cos\Psi$$

z' = z

$$\begin{bmatrix} x' \\ y' \\ z' \end{bmatrix} = Rz\,\Psi \begin{bmatrix} x \\ y \\ z \end{bmatrix} \text{ and } Ry\theta = \begin{bmatrix} \cos\Psi & -\sin\Psi & 0 \\ \sin\Psi & \cos\Psi & 0 \\ 0 & 0 & 1 \end{bmatrix}$$

B) Considering the second rotation θ (pitch) around the y-axis:

Considering angle θ with respect to the x-axis.

$$x' = OA - BC$$
$$= x\cos\theta - z\sin\theta$$
$$z' = AB + CP$$
$$= x\sin\theta + z\cos\theta$$

y' = y

$$\begin{bmatrix} x' \\ y' \\ z' \end{bmatrix} = Ry\theta \begin{bmatrix} x \\ y \\ z \end{bmatrix} \text{ and } Ry\theta = \begin{bmatrix} \cos\theta & 0 & -\sin\theta \\ 0 & 1 & 0 \\ \sin\theta & 0 & \cos\theta \end{bmatrix}$$

C) And for the third rotation φ(roll) around the x-axis:

Considering angle Φ with respect to z- axis.

$$x' = x$$
$$y' = AB + CP$$
$$y' = y\cos\Phi + z\sin\Phi$$
$$z' = OA - BC$$
$$z' = z\cos\Phi - y\sin\Phi$$

$$\begin{bmatrix} x' \\ y' \\ z' \end{bmatrix} = Rx\Phi \begin{bmatrix} x \\ y \\ z \end{bmatrix} \text{ and } Rx(\Phi) = \begin{bmatrix} 1 & 0 & 0 \\ 0 & \cos\Phi & \sin\Phi \\ 0 & -\sin\Phi & \cos\Phi \end{bmatrix}$$

The full rotation matrix of the base relative to the platform is then given by:

$^{b}Rp = Rz(\Psi)\, Ry(\theta)\, Rx(\varphi)$

bRp =

$$\begin{bmatrix} \cos\Psi\cos\theta & -\sin\Psi\cos\Phi + \cos\Psi\sin\theta\sin\Phi & -\sin\Psi\sin\Phi - \cos\Psi\sin\theta\cos\Phi \\ \sin\Psi\cos\theta & \cos\Psi\cos\Phi + \sin\Psi\sin\theta & \cos\Psi\sin\Phi - \sin\Psi\sin\theta\cos\Phi \\ \sin\theta & -\cos\theta\sin\Phi & \cos\theta\cos\Phi \end{bmatrix}$$

Now consider a Stewart platform:-

The coordinate qi of the lower anchor point bi with respect to the platform is given by the equation

$$q_i = \bar{T} + BRP \times \bar{bi}$$

Where,

- $\bar{T}$ is the translation vector, giving the positional linear displacement of the origin of the Base frame with respect to the Platform, and
- $\bar{bi}$ is the vector defining the coordinates of the lower anchor point bi with respect to the base framework.

Since $\bar{qi} = \bar{T} + pRB \times \bar{bi} = \bar{pi} + \bar{li}$

So the length of ith leg is given by

$$li = \bar{T} + pRB \times \bar{bi} - \bar{pi}$$

Where $\bar{bi}$=vector defining the co-ordinate of lower anchor point bi.

Assume $\bar{u}$ be co – ordinate of base plate center with respect to upper anchor point pi which is given by

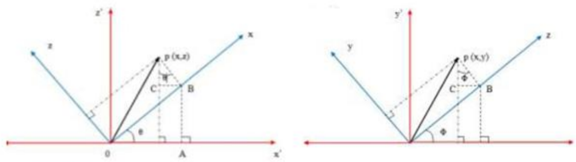

Fig.8 1 Rotation of base about z-axis   Fig.8 .2 Rotation of base about y-axis

$ui = \bar{T} + pi.$

Since we are using servomotor a further calculation is required to determine the angle of rotation of the servo.

Where, a=length of the servo operating arm.

AI are the points of arm on ith servo with co-ordinates.

$$a = \begin{bmatrix} xa \\ ya \\ za \end{bmatrix}$$

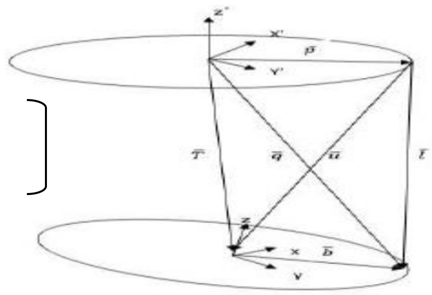

Fig.9 Rotation of base about x-axis

In the base framework. Bi are the points of rotation of the servo arm with co-ordinates.

$$b = \begin{bmatrix} xb \\ yb \\ zb \end{bmatrix}$$

In the base framework. Pi is the point that joints between the operating rods and the platform with coordinates

$$p = \begin{bmatrix} xp \\ yp \\ zp \end{bmatrix}$$

In the base framework.

S=length of the operating leg

α=angle of servo operating arm from horizontal

β=angle of servo arm relative to x-axis

Point A is constrained to be on servo arm but arrangement of servo motor should be such that even and odd motor arm should b reflection of each other. So for even legs we have

$xa = a\, cos\alpha\, cos\beta + xb$
$ya = a\, cos\alpha\, sin\beta + yb$
$za = a\, sin\alpha + zb$
And for the odd legs we have,
$xa = a\, cos(\pi - \alpha)\, cos(\pi + \beta) + xb$
$ya = a \cos(\pi - \alpha) \sin(\pi + \beta) + yb$
$za = a \sin(\pi - \alpha) + zb$
But $sin(\pi - \alpha) = sin\alpha$ and $sin(\pi + \beta) = -sin\beta$
$cos(\pi - \alpha) = -cos\ \alpha$ And $cos(\pi + \beta) = -cos\beta$
Therefore,
$xa = a\, cos\alpha\, cos\beta + xb$
$ya = a\, cos\alpha\, sin\beta + yb$
$za = a\, sin\alpha + zb$
$\bar{A} = \bar{b} + \bar{a}$
$\bar{a} = \bar{A} - \bar{b}$
$a^2 = (xa + xb)^2 + (ya + yb)^2 + (za + zb)^2$
$= (xa^2 + ya^2 + za^2) + (xb^2 + yb^2 + zb^2) - 2(xa\, xb + ya\, yb + za\, zb)$ (14)

Now $\bar{l} = \bar{u} + \bar{b}$
$l^2 = (xu + xb)^2 + (yu + yb)^2 + (zu + zb)^2$
$= (xu^2 + yu^2 + zu^2) + (xb^2 + yb^2 + zb^2) - 2(xu\, xb + yu\, yb + zu\, zb)$ (15)

Now $\bar{s} = \bar{u} + \bar{a}$
$s^2 = (xu + xa)^2 + (yu + ya)^2 + (zu + za)^2$
$= (xu^2 + yu^2 + zu^2) + (xa^2 + ya^2 + za^2) - 2(xu\, xa + yu\, ya + zu\, za)$ (16)
From equation (2.1), (2.2) and (2.3)
$s^2 = l^2 - (xb^2 + yb^2 + zb^2) - 2(xu\, xb + yu\, yb + zu\, zb) + a^2 - (xb^2 + yb^2 + zb^2) + 2(xa\, xb + ya\, yb + za\, zb) + 2(xu\, xa + yu\, ya + zu\, za)$
Which is an equation of the form
$L = M \sin\alpha + N \cos\alpha$
Using the trigonometry for the sum of sine waves
$a \sin\alpha + b \cos\alpha = c \sin(x + \gamma)$
Where $c = \sqrt{a^2 + b^2}$ and $\tan y = (a/b)$
We therefore have another sine function of a with a phase shift of δ
$L = [\sqrt{(M^2 + N^2)}]\sin(\alpha + \delta)$
Where $\delta = \tan^{-1}(N/M)$
And $\alpha = \sin^{-1}(L/\sqrt{M2 + N2}) - \tan^{-1}(N/M)$
Where $L = s^2 - (l^2 + a^2)$
$M = 2a(Z_b + Z_u)$
$N = 2a[\cos\beta(xb + xu) + \sin\beta\,(yb + yu)]$ [17]

Experimental Setup

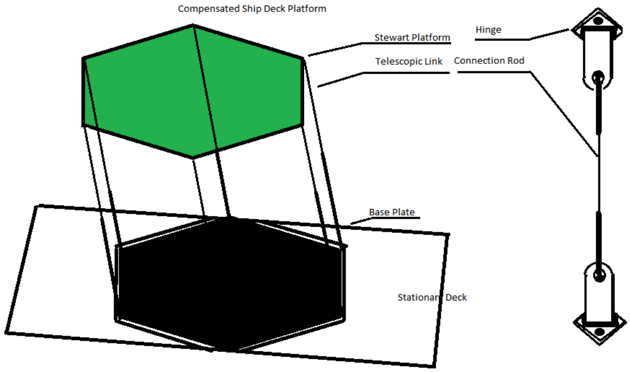

Fig. 10 – Compensated Ship Deck Platform using Stewart Platform

The experimental setup consists of one fixed platform and one mobile platform. The mobile platform is hexagonal in shape. Each joint is connected with hinge joints. The top platform and bottom fixed platform are connected with each other using telescopic connecting rods of varying lengths. Each connecting rod at the hinge joint on the fixed platform is fixed to servo motors individually. The experimental setup involves getting the sinusoidal wave as input from the Sine Summation Fit Algorithm. Owing to the input sinusoidal wave; the mobile platform must remain at all times stable such that the launch and recovery of the UAVs is achievable. The upper mobile platform or stewart platform must compensate the ships movements.

IV. POSITION CONTROL

Control stage is based on a Arduino Mega 2460 microcontroller sensor array. The Sensor Array is connected to PC using Serial Programming, where the controller can be easily programmed. The control law is introduced in Arduino IDE environment, then compiled and downloaded to Arduino sensor array using real time tools. The controller card captures voltage signals from inertial measure unit, length sensor and motor encoders. It also calculates every three millisecond new control signal and feeds the motor amplifiers and the air piston proportional valves. Control position for both platforms (i.e. SP and AH) is performed through proportional derivative PD controllers so as to assure stability even with errors in steady state. These PD gains for electric motors and for pneumatic proportional valves are tuned experimentally. It is important to consider that due compressive air properties, air pistons' behavior is different when moving up or moving down. Therefore, two different PD gains are set to each pneumatic piston.

ACKNOWLEDGMENT

I, D.Ravi Vikranth, First Author would like to acknowledge and thank Prof. Anurag Sarma and Prof. Brijesh Patel, Principal for their encouragement in completing this paper. I would also like to take this opportunity to thank all teaching and non – teaching staff of the Department for their valuable support.

REFERENCES

[1] Gauri N. Parkar, Sandeep R. Singh, Alok J. Singh et.al.,"Design, Manufacturing and Testing of Ship Deck Motion Compensation Platform by using Stewart Platform", IJCRT, Vol. 6, Issue 1, ISSN: 2320-2882, March' 2018, pp 1165-1170

[2] Christian Bolander, Douglas Hunsaker, " A Sine Summation Algorithm for prediction of Ship Deck Motion", Conference Paper DOI: DOI: 10.1109/OCEANS.2018.8604888, October' 2018, ResearchGate ref. : https://www.researchgate.net/publication/327868083

[3] Alexdandre Campos, Jacqueline Quintero, "An Active Helideck Testbed for Floating Structures based on Stewart Gough Platform", IEEE/ RSJ International Conference on Intelligent Robots & Systems, France, Sept' 2008, pp 3705-3710.

[4] R A Ibrahim, I M Grace, "Modeling of Ship Roll Dynamics and its coupling with Heave and Pitch", Mathematical Problems in Engineering, Hindawi Publishing Corporation, Vol. 10, Article ID 934714, DoI:10.1155/2010/934714

[5] Aung Myat Thu, Ei Ei Htwe, Htay Htay Win, "Mathematical Modeling of a Ship Motion in Waves under Coupled Motions", International Journal of Engineering and Applied Sciences, ISSN: 23943661, Vol. 2, Issue 12, Dec.' 2015, pp 97-102